Rapid Screening of Genetic Biomarkers of Infectious Agents Using Quantum Dot Barcodes

Supratim Giri, Edward A. Sykes, Travis L. Jennings, and Warren C. W. Chan*

Institute of Biomaterials and Biomedical Engineering, Terrence Donnelly Centre for Biomolecular Research, Materials Science and Engineering, Chemical Engineering, Chemistry, University of Toronto, 164 College Street, Toronto, Ontario, M5S 3G9, Canada

ABSTRACT The development of a rapid and sensitive infectious disease diagnostic platform would enable one to select proper treatment and to contain the spread of the disease. Here we examined the feasibility of using quantum dot (QD) barcodes to detect genetic biomarkers of the bloodborne pathogens HIV, malaria, hepatitis B and C, and syphilis. The genetic fragments from these pathogens were detected in less than 10 min at a sample volume of 200 μL and with a detection limit in the femtomol range. A next step for the advancement of QD barcode technology to the clinic will require validation of the technology with human samples to assess for matrix effects, head-to-head comparison with existing detection method, development of techniques to automate the assay and detection process, and simplification of analytical device for the read-out of the barcode signal. Our study provides an important intermediate step in the translation of QD barcode technology for screening infectious disease agents in the developed and developing world.

KEYWORDS: quantum dots · global health · infectious diseases · nanotechnology · diagnostics · DNA · multiplexing · barcodes

Infectious diseases are the number one cause of global mortality. There is currently a global challenge to develop point-of-care diagnostic platforms for detection of the pathogens responsible for the diseases.[1−3] Infectious diseases could start in one region of the world and rapidly spread through air, water, human, or animal contact.[3] The development of rapid and sensitive point-of-care diagnostics can prevent the spread of the disease since detection would enable one to select the proper treatment for the disease or quarantine patients. The current gold standards in diagnosing infectious diseases include microscopy, cultures, enzyme-linked immunoassays, and lateral flow immunoassays.[4−6] Concerns over the accuracy, speed of analysis, and the limited ability of these techniques to detect multiple strains or infectious disease agents have encouraged researchers to consider alternative molecular diagnostic platforms.[1] The technique of polymerase chain reaction, better known as PCR, is now being optimized for infectious disease diagnostics and has advanced toward clinical utility.[7] The disadvantages of this technique are their higher cost, slower speed of analysis, and technical or operational complexity.[8−10] Furthermore, the disadvantages of each of these techniques preclude their use in the developing world. Therefore researchers have started to evaluate emerging technologies such as microfluidics and barcoding strategies for infectious disease diagnostics.[11,12]

Barcoding technologies have gained popularity for applications in biomolecular detection in the last five years because of the commercial availability of the Luminex system.[13] Microbeads are encoded with fluorescent organic dye molecules of different wavelengths and intensities to create a library of barcodes for the multiplex detection of target molecules. The doping of microbeads with organic fluorophores has limitations because organic fluorophores have broad fluorescence spectra (>55 nm) and microbeads doped with multiple organic fluorophores typically require multiple lasers for excitation. This has made the instrumentation costly and bulky. In addition, the spectral overlap of organic fluorophores limits the number of useful barcodes to 100 or less. New strategies involving barcodes have been proposed to overcome the limitations of organic fluorescent molecules for coding. Optical (*e.g.*, quantum dot and Raman signature-based barcodes),[14−16] graphical (*e.g.*, striped metallic structures or etched polymer matrix or barcoded polymeric hydrogel),[17−19] or molecular (*e.g.*, DNA)[20] signatures have all been considered. Microbead-based barcodes would make the fastest impact in diagnostics of infectious agents because this is the most mature barcode platform.[21,22] In addition, the procedures to scale up production of microbeads and the conjugation chemistry of targeting agents onto the microbead surface are well established. As

* Address correspondence to warren.chan@utoronto.ca.

Received for review October 26, 2009 and accepted February 8, 2011.

Published online February 28, 2011
10.1021/nn102873w

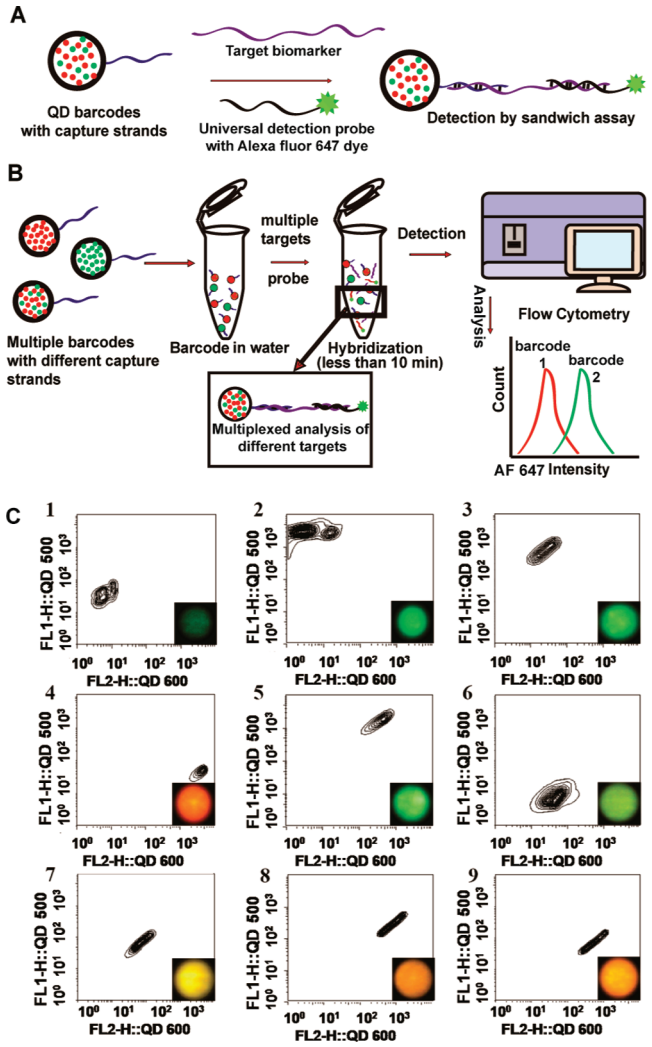

Figure 1. Schematic diagram of QD barcode assay. (A) The basic principles of detection in direct assay. (B) Flowchart shows the sequential steps involved in the assay. (C) Barcode library showing 2-dimensional contour map plots obtained from flow cytometry study. The numbers shown at the top left corner of each plot correspond to the individual barcodes. Fluorescence microscopy image of each microbead was also provided with the corresponding contour plot. The x and y axis refers to the fluorescence intensities of 500 and 600 nm emitting QDs, respectively. FL-H refers to the fluorescence intensity.

a result, the translation of microbead-based barcodes into commercially useful clinical panels for biomedical detection of infectious diseases, cancer, and cardiovascular diseases would be the fastest.

Quantum dots are a natural replacement for organic fluorophores for doping microbeads to create barcodes.[14] They have many advantages over organic fluorophores for doping microbeads to generate unique optical barcodes. Quantum dots have a narrower spectral line width than organic fluorophores, different emissions can be excited with a single wavelength, and the emission wavelength is tunable by size, composition, and shape.[23] Unfortunately, synthetic and signal deconvolution challenges have prevented this technology from advancing from the academic laboratory to a commercially viable technology for clinical analysis. Recently, we overcame some of the synthetic challenge of creating QD barcodes by using the continuous flow focusing technique to create over 100 different barcodes by using combinations of different emitting QDs.[24] Furthermore, proteins or oligonucleotides have been successfully coated onto the microbead's surface using carbodiimide chemistry.[24] By having the capability to prepare QD barcodes reproducibly, the next step is to optimize and characterize parameters that dictate their assay performance. Here, we investigated the sensitivity ranges and hybridization kinetics of QD barcode-based assay as well as assessed the capability of QD barcodes for multiplex analysis of gene fragments of five bloodborne infectious agents (*e.g.,* SK102 sequence for *gag* region of HIV-1 genome, PB1 sequence for Pre-C and C regions of HBV genome, *etc.*). This is an intermediate but important step toward the eventual use of this technology in the clinic and the implementation of QD barcodes in point-of-care diagnostic platforms.

RESULTS AND DISCUSSION

We characterized the detection sensitivity, kinetics, and cross-reactivity of QD barcodes for detecting

TABLE 1. Barcode Nomenclature and Corresponding Capture Strand Sequence

barcode	relative intensity (500 nm:600 nm)	capture strand sequence code	capture Sequence (5′ to 3′)[a]	targeting biomarker for
1	15:1	C1	AAT ATA TTT GGT TTT CCC AAA CCA GTT TAA	rFAL1 - P. Falciparum Malaria
2	285:1	C2	AAA AAA AAA ACG TCC TTT GTC TAC GTC CCG	Hepatitis B (HBV)
3	80:2	C3	GAG ACC ATC AAT GAG GAA GCT GCA GAA TGG GAT	SK102 HIV-1
4	7:630	C4	CAT AGT GGT CTG CGG AAC CGG TGA GT	KY 150 Hepatitis C (HCV)
5	220:55	C5	CTT TAT AAG GAT CAA TGT CCA TGC	PB-3 HBV
6	1:12	C6	TCA GAA GGC AAA AAA GAG AGT AAC T	PB-2 HBV
7	18:18	C7	GAC AAT GCT CAC TGA GGA TAG T	T. pallidum 47-1
8	100:250	C8	ACG CAC AGA ACC GAA TTC CTT G	T. pallidum 47-2
9	30:200	C9	TTG TGG TAG ACA CGG TGG GTA C	T. pallidum 47-3

[a] All oligonucleotides are functionalized with NH_2 group at the 5′ end.

TABLE 2. Barcode Nomenclature and Corresponding Capture Strand Sequence

barcode	capture strand sequence code	target strand sequence code	target sequence (5′ to 3′)	secondary detection probe linked with AF 647 at 5′ end (SA) (5′ to 3′)
1	C1	T1	CGG CGA TGA ATA CCT AGG ACA CTT ACT ATT AAA CTG GTT TGG GAA AAC CAA ATA TAT T	TAA GTG TCC TAG GTA TTC ATC GCC G
2	C2	T2	CGG CGA TGA ATA CCT AGG ACA CTT ACT ACG GGA CGT AGA CAA AGG ACG TTT TTT TTT T	
3	C3	T3	CGG CGA TGA ATA CCT AGG ACA CTT ACT AAT CCC ATT CTG CAG CTT CCT CAT TGA TGG TCT C	
4	C4	T4	CGG CGA TGA ATA CCT AGG ACA CTT ACT AAC TCA CCG GTT CCG CAG ACC ACT ATG	
5	C5	T5	CGG CGA TGA ATA CCT AGG ACA CTT ACT AGC ATG GAC ATT GAT CCT TAT AAA G	
6	C6	T6	CGG CGA TGA ATA CCT AGG ACA CTT ACT AAG TTA CTC TCT TTT TTG CCT TCT GA	
7	C7	T7	CGG CGA TGA ATA CCT AGG ACA CTT ACT AAC TAT CCT CAG TGA GCA TTG TC	
8	C8	T8	CGG CGA TGA ATA CCT AGG ACA CTT ACT AAG CCT AAG CTT GTC AGC GAT CA	
9	C9	T9	CGG CGA TGA ATA CCT AGG ACA CTT ACT AGT ACC CAC CGT GTC TAC CAC AA	

nine different gene fragments from syphilis, HIV, malaria, hepatitis B, and hepatitis C genome simultaneously. These pathogens contribute to the highest mortality across the world and current methods to diagnose each of these pathogens are relatively slow.[1−3] Syphilis (T. pallidum) was included in this panel because it has strong links to HIV co-occurrence. The selected gene fragments are commonly used primers or probes for RT-PCR analysis of the selected pathogens.[25−27]

Experimental Conditions. QD barcodes are conjugated with single-stranded oligonucleotides (capture strands) that can hybridize to a target sequence. In our case, this target sequence is from a gene fragment from one of five pathogens. This target sequence can also hybridize onto a secondary oligonucleotide that is conjugated with the dye Alexa Fluor 647 (λ_{ex}= 647 nm, λ_{em}= 667 nm) (Figure 1A). The optical signature of the barcode created by using two different emitting QDs (500 and 600 nm) identifies the target sequence since different capture strands are coated onto different emitting QD barcodes. A library of QD barcodes conjugated with capture strands is placed into a vial along with the secondary oligonucleotide-Alexa Fluor 647 conjugate (denoted as SA). When we introduce a target sequence into the vial, that target recognizes both the QD barcodes and the SA, thereby assembling the QD barcode and SA together (Figures 1A and 1B). By measuring the optical emission of this assembled complex in a flow cytometer, a positive detection is observed when a fluorescence signal arises from both the QDs inside the microbeads and Alexa fluor 647 at the same time.

The target sequences we used as biomarkers were synthetic oligonucleotides, mimicking short genetic fragments of pathogens (Tables 1 and 2). This type of synthetic genetic biomarkers are typically used in proof-of-concept studies of newly developed DNA diagnostics.[19,28−31] We conducted our experiments in 10 mM PBS (pH 7.4) containing 0.1% Tween. A number of genetic assays including RT-PCR have been reported to be carried out in serum or blood free media containing phosphate or Tris buffer, $MgCl_2$, 0.1% Triton, *etc.*[19,28,32−36] In clinical studies, DNA or RNA is normally extracted from blood or plasma samples prior to PCR analysis in aqueous buffers.[25−27] Therefore, we did not feel necessary to validate our system for samples in blood or serum at this point.

QD Barcode Preparation. Nine unique barcodes were prepared using continuous flow focusing for this study.[24] The barcodes were prepared by mixing a combination of two different emitting QDs (500 and 600 nm) with the polymer poly(styrene-*co*-maleic anhydride) in chloroform. This solution was introduced into a flow focusing nozzle system using a syringe pump. Water was used as the focusing fluid. Microbeads are created at the tip of the nozzle from the microfluidic instability. After the microbeads pinch off from the tip, the anhydride functional groups on the microbeads hydrolyze to carboxylic acid functional groups. The optical signal from the QDs is a reflection of concentration of the QDs in solution. For example, if the solution contains three different emitting QDs, the

microbead will contain three different fluorescence emissions. However, the intensities of the microbead fluorescence may be different than in solution because the QDs are packed into a more confined space and fluorescence resonance energy transfer may occur. To ensure that the nine QD barcodes can be optically differentiated from one another, we adjusted the ratios of the different QDs in solution, prepared the barcodes, and then used flow cytometry to determine whether they can be differentiated from one another. Figure 1C shows a 2-dimensional contour diagram of the nine different barcodes used in this study. In our flow cytometry measurement, we used 520 ± 40 nm (denoted as FL1) and 585 ±42 nm (denoted as FL2) bandpass filters to differentiate the two QD emission signal. These microbeads had an average size of 5 ± 1 μm. Previously, we characterized the detailed physical and chemical properties and stability of these barcodes in different temperatures, salts, and pH values and the methodologies used in this study were similar.[24] We stored our QD barcodes and used them according to the defined parameters of our previous study.[24]

Conjugation of Oligonucleotides to QD Barcodes. A water-soluble carbodiimide reaction was used to conjugate amine-terminated oligonucleotides to the carboxylic acid function groups on the QD barcode surface. The oligonucletoide was linked to the QD barcode *via* an amide bond. Each barcode was assigned to a specific oligonucleotide capture strand, indicated in Table 1. We selected the sequences of the capture strands from primers or probes commonly used for RT-PCR amplification of the specific regions of genomic DNA corresponding to the respective pathogens mentioned in Table 1.[25−27] A direct assay was used to determine whether the surface was successfully coated with the oligonucleotide. In a model study, QD barcode 4 was conjugated with various amounts of a capturing oligonucleotide sequence (C4) and was tested against a fixed concentration of complementary oligonucleotide sequence directly attached to the organic dye Alexa Fluor 647 (Supporting Information, Figure S1).

Our experiment showed that we are not able to obtain a measurable signal form the Alexa Fluor 647 when we added less than 1 pmol of capture strand per million beads on the QD barcode surface for conjugation. We speculate that the anchored capture strand sequences, which are responsible for the interaction between the bead surface and any complementary sequence, are not available for hybridization. With a lower capture strand density, the ability of a target to bind to the beads gets mitigated.[37] However, excess capture strands can also inhibit the hybridization to a complementary sequence due to steric effects.[37] We determined that the upper limit to be 100 pmol of capture strands per million beads. In all subsequent studies, we used 10 pmol capture strands per million QD barcoded beads for the assay because the hybridization kinetics and multiplexing capability of the QD barcodes were not affected at the optimal range of 1 pmol to 60 pmol capture strands per million barcodes. The only factor to be affected is the analytical sensitivity. By reducing the concentration of the capture strand, we also reduce the cost of preparing the barcodes.

Hybridization Kinetics of QD Barcodes. We measured the hybridization kinetics of QD barcode assays to determine the rate and amount of time required for the QD barcode assay to reach completion. We used QD barcode 4 as a model barcode for all of the singleplex experiments. Target sequence (T4) and the SA were added to the QD barcode 4 conjugated with capture strand (C4), and the sample was measured by flow cytometry at a 10 s time interval. Figure 2A shows that Alexa Fluor 647 dye signal increases with time exponentially. This hybridization process of QD barcodes appears to have first-order kinetics. The curve is fit to the equation

$$I(t) = A(1 - e^{-kt}) + c$$

Where A is the pre-exponential weight for each process, k is the associated hybridization rate constant, and $I(t)$ is the observed normalized intensity at time t.

Our results show that the hybridization rate constant involving barcode, target, and capture strand is 3.39×10^{-3} per second with a half-life of 204 s (Table 3). We determined that the hybridization rate for our QD barcode assay is slower than the hybridization of a pair of oligonucleotides-only.[38] Gao *et al.* reported a 100% hybridization efficiency of 5 min for a 25 base pair double stranded DNA. However, the hybridization reaction is 20 to 40 fold slower when the hybridization reaction of DNA duplexes occurs on a flat gold surface using surface plasmon resonance for detection.[39] However a complete hybridization on flat surfaces requires hours instead of minutes.[40] We estimate that our hybridization rate is at least 10−20 times faster than heterogeneous assays and is likely to be slower than hybridization of unbound DNA only. Our observed faster kinetics in comparison to heterogeneous assays stem from the ability of microbeads to diffuse in solution and to constantly refresh their depletion layer (volume of low analyte concentration immediately around the reactive surface).

Detection Sensitivity. We determined the detection limit of our QD barcode assay using QD barcode 4 as a model. The sample vial was incubated with capture strand conjugated QD barcode 4, target (T4), and SA for 10 min and at a volume of 200 μL. Based on the hybridization kinetics, 10 min ensured a completed reaction. We observed a detection limit of 100 fmol (Figure 2B), 1 fmol (Figure 2C), and 10 fmol (Figure 2D) when barcode 4 was conjugated with 1 pmol, 60 pmol, and 10 pmol of capture strands per million beads, respectively. Therefore, the limit of sensitivity and the linear dynamic range of detection are dependent on the amount of capture strand conjugated to the microbead's surface. The different coverage of surface

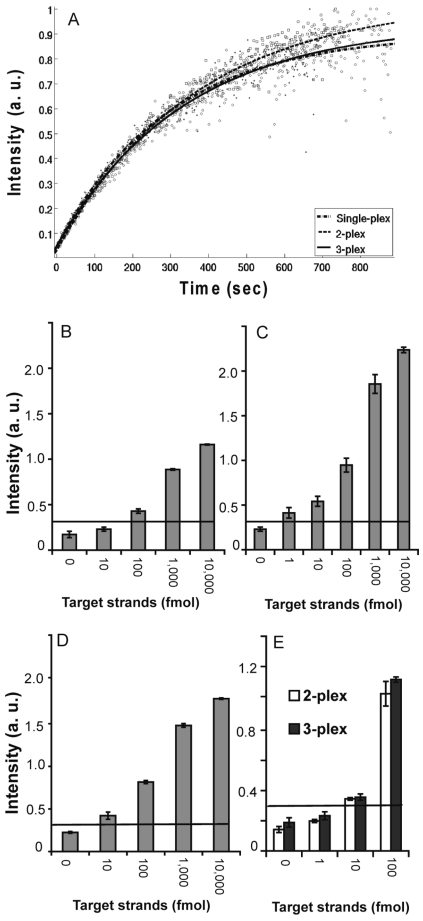

Figure 2. Assessing hybridization kinetics and detection sensitivity using barcode 4 by flow cytometry. Fluorescence intensity of Alexa Fluor 647 dye was plotted in *y* axes. (A) Kinetic plots of intensity of fluorescence due to DNA hybridization *vs* time. An increase in the fluorescence intensity shows that the targeting sequence binds to the capture strands on the barcode and the secondary target-conjugated with Alexa Fluor 647. The parameters of the flow cytometer are set to measure the Alexa Fluor 647 dye molecule. Barcodes used: 4 for single-plex; 4 and 6 for 2-plex; 4, 6, and 8 for 3-plex. (B) Sensitivity plot using 1 pmol of capture strand per million beads. (C) Sensitivity plot using 60 pmol of capture strand per million beads. (D) Sensitivity plot using 10 pmol of capture strand per million beads. (E) Effect of multiplexing on sensitivity, using 10 pmol of capture strand per million beads. Horizontal solid line shows the minimum detection threshold, which is 3 standard deviations above the negative control. Error bars were calculated on the basis of independent assays in triplicates.

capture strands accounts for the adjustable sensitivity, which could be important for minimizing false positive results.

Multiplex Detection. The ability to detect multiple biomarkers in the same sample is critical to rapid diagnosis. To provide perspective, in a typical microbial culturing experiment, every sample has to be individually cultured and each sample has to be analyzed on a microscope by a skilled technician. The ability to detect multiple genetic markers in a small volume in less than 10 min would accelerate the diagnostic process and enable physicians to make treatment decisions more rapidly. While we have already shown that the hybridization kinetics is rapid, a demonstration of multiplex detection using multiple barcodes in a single vial would significantly speed up the diagnostic process. First, we evaluated whether the presence of multiple barcodes would affect the hybridization kinetics and sensitivity. Figure 2A shows that the hybridization for QD barcode 4 for a 2-plex (where barcodes 6 and 4 were combined in the sample vial to detect both T6 and T4, respectively) and a 3-plex assay (where barcodes 6, 8, and 4 were combined to detect T6, T8, and T4, respectively), was not significantly different in terms of rate and reaction completion time ($p > 0.05$, *t* test comparison) (see Table 3). Similarly, in Figure 2E, the detection limit of QD barcode 4 (10 fmol) was not affected by the presence of QD barcode 6 (2-plex assay) and QD barcodes 6 and 8 (3-plex assay) in the sample vial.

TABLE 3. Hybridization Kinetics of QD Barcodes

barcode combination	type	hybridization rate constant k (10^{-3} s^{-1})[a]
4	single-plex	3.39 ± 0.72
4, 6	2-plex	2.75 ± 0.34
4, 6, 8	3-plex	2.97 ± 0.51

[a] Rate constant of barcode 4 is reported in each case.

Finally, we determined the use of nine barcodes to detect nine genetic markers in the same vial. A buffer solution was incubated with all nine capture strand-conjugated QD barcodes. After spiking all nine target biomarkers and SA and an incubation period of 10 min we demonstrate the detection of all nine gene fragments simultaneously (Figure 3A). In contrast, no measurable signal was observed for solutions containing no biomarker targets (Figure 3B). To determine if cross-reactivity can occur, we purposely spiked the buffer with different genetic targets. In Figure 3C, we spiked the buffer with sequences T1, T3, T5, T7, and T9. Our experiments show that the QD barcodes are able to distinguish the gene fragments present in the buffer *versus* ones that are not. To further validate the ability of the QD barcodes to select and measure the different combination of genetic fragments, different combinations were conducted (Figure 3D–F). The limit of detection in each case was 10 fmol (Figure 3A–F). These results conclusively demonstrate the ability of QD barcodes to selectively detect a multitude of different genetic sequences in buffer simultaneously.

CONCLUSION

The unique health care needs of the developing world, and the recent spread and scare of the H1N1 and SARS virus highlight the urgency in designing and engineering rapid and multiplex diagnostics. Currently, there is a global challenge to develop cost-effective and rapid diagnostic platforms for infectious pathogens. Our results suggest that QD barcodes may be a viable diagnostic platform for infectious disease detection. This technology

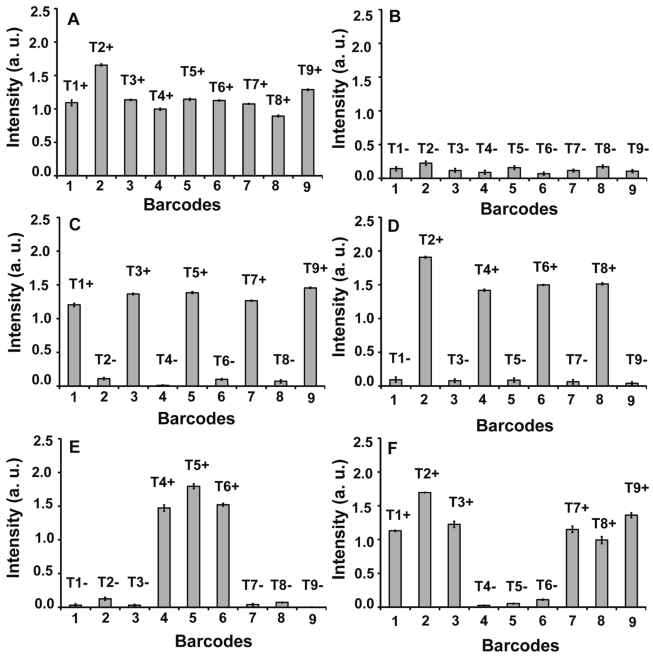

Figure 3. Assessing multiplexed detection specificity. All nine barcodes conjugated with the respective capture strands were used in all multiplexed detection experiments and "+" and "−" symbol represents presence and absence of targets, respectively (A−F). All targets were present and detected (A). No targets were detected in the control experiment (B). Targets T1, T3, T5, T7, and T9 were detected only when those targets were present (C). Targets T2, T4, T6, and T8 were detected only when those targets were present (D). Targets T4, T5, and T6 were detected only when those were present (E) and T1, T2, T3, T7, T8, and T9 were detected only when those were present (F). Error bars were calculated based on independent assays in triplicates.

has demonstrated versatility in detecting both genomic and proteomic biomarkers, and the barcodes could be simply measured and detected using flow cytometry.[24] However, flow cytometry may have limited use in point-of-care situations because of their large size and cost. There is effort in creating a miniaturized QD barcode detection system using microfluidics in combination with laser induced fluorescence for use at point-of-care.[11]

As a step toward fulfilling the global challenge, we examined the feasibility of molecularly detecting infectious pathogens using QD barcodes. Here, we show that the detection of gene fragments from infectious agents requires less than 10 min and a sample volume of less than 200 μL. Additionally, nine different genetic fragments can be detected using nine different QD barcodes with high fidelity. The combination of fast hybridization kinetics on QD barcodes with multiplexing provides a speed advantage of the QD barcode technology over traditional diagnostic methods such as cell culturing and immunochromatographic strip tests. The lowest limit of our detection (1 fmol) was calculated to be 16.5 pg for a 54 bp DNA fragment, which was comparable to that of Mahoney and coworkers who reported a limit of detection of 0.2 ng of genomic DNA (200 bp) using a QD barcode-based detection system.[41] In comparison to other emerging technologies such as the biobarcode-amplification technology using scanometric detection created by Mirkin's group or the graphical barcodes created by Doyle's group, our reported sensitivity is approximately 100 times poorer.[19,28] However, both Mirkin and Doyle in their methods required a minimum of 3 h to conduct the assay. Our study presents a method to detect DNA fragments at room temperature within minutes without the requirement of any washing or heating/cooling cycles (in comparison to PCR) while maintaining excellent fidelity for up to 9-plex assay. Currently, we are continuing to improve the analytical sensitivity by optimizing various parameters such as length of capture strands, temperature of hybridization, incubation time, and use of various fluorescence enhancement techniques.[42]

In essence, we demonstrated the capability of QD barcodes to detect nine different gene fragments stemming from five different infectious pathogens in a single sample volume and in a rapid fashion. As a next step in the development process, the ability of QD barcodes to detect genetic markers from clinical samples should be conducted to assess the effect of biological matrix on assay performance. With clinical samples, many of the nucleic acid sequences of interest may be larger than 200 bp. A larger-sized DNA sequence could impact the hybridization kinetic, analytical sensitivity, and dynamic range using QD barcodes for detection due to the possible formation of secondary structures. A possible solution to this problem would be enzymatic degradation of the longer sequences into shorter fragments prior to detection. Our previous study demonstrated that longer sequences cut into shorter fragments by

endonucleases can be easily detected using QD barcodes.[42] Finally, to further integrate QD barcodes in a point-of-care diagnostic platform, there is the need to automate the process of extracting and isolating the genetic sequence of interest from clinical samples and the assays and to develop a cost-effective miniaturize QD barcode read-out device to replace the flow cytometer.

METHODS

Synthesis of QDs. ZnS-Capped CdSe QDs were synthesized and characterized according to previously published procedures and stored in chloroform until further use.[43−45]

Fabrication of QD Barcoded Polymeric Microbeads. Barcodes were prepared by mixing different wavelength emitting QDs (500 and 600 nm) and the polymer poly(styrene-*co*-maleic anhydride) in chloroform. The resulting solution was then introduced into a nozzle system (Ingeniatrics) using a syringe pump (World precision Instruments) at a rate of 1 mL/h along with the focusing fluid water. The entire nozzle system was then submerged inside a beaker partially filled with water. The polymeric barcoded microbeads were synthesized *in situ*, and the beads formed a white colloidal suspension in the water. After the synthesis, the valve was closed and the beads were hardened by an overnight stirring and then collected. The microbeads were then filtered using 35 μm BD Falcon nylon mesh strainer cap, counted using an automated (Beckman Coulter) Vi-Cell counter. The relative intensities of the barcoded beads were varied by changing the concentrations of the two different wavelength emitting QDs in chloroform. The concentrations of QDs in chloroform for each of the barcodes used were 5.9 μM of 500 nm and 0 μM of 600 nm for barcode 1, 25.0 μM of 500 nm and 0 μM of 600 nm for barcode 2, 13.8 μM of 500 nm and 0 μM of 600 nm for barcode 3, 1.0 μM of 500 nm and 6.8 μM of 600 nm for barcode 4, 22.2 μM of 500 nm and 1.0 μM of 600 nm for barcode 5, 0 μM of 500 nm and 0.82 μM of 600 nm for barcode 6, 4.5 μM of 500 nm and 1.0 μM of 600 nm for barcode 7, 12.5 μM of 500 nm and 4.1 μM of 600 nm for barcode 8, and 2.9 μM of 500 nm and 4.1 μM of 600 nm for barcode 9.

Conjugation of Capture Strands on the Surface of Polymeric Microbeads. The carboxylic acid groups present on the surface of polymeric microbeads were conjugated with the amine groups present at the 5′ end of the DNA capture strands. DNA strands were purchased HPLC-purified from IDT DNA Technologies and used without further purification. In a typical experiment, 5.0×10^{-11} moles of a specific capture strand DNA was added to a corresponding 5.0×10^6 microbeads (approximate number of beads were counted in automated Vi-cell counter) of the specific barcode suspended in 500.0 μL of MES buffer in pH 5.3 in the presence of 6.25×10^{-5} moles of EDC (1-ethyl-3-(3-dimethylaminopropyl) carbodiimide hydrochloride). The mixture was stirred overnight followed by the addition of 300 μL of 0.1% (by volume) of Tween in PBS to the beads followed by centrifugation. The supernatant was removed, an additional 500 μL of 0.1% (by volume) Tween in PBS was added, and the beads were stored at 5 °C.

Variation of Capture Strand Coverage on Microbeads. We followed our previously published literature procedure to conjugate different pmols of DNA capture strand on the microbead surface.[24,37] In a typical experiment, 1 million microbeads of barcode 4 (approximate number of beads were counted in automated Vi-cell counter) was added each in seven different individual Eppendorf tubes, and 0, 1, 5, 10, 40, 60, 100 pmols of capture strand (C4) were added, respectively, in each individual tube in the presence of 500 μL of MES buffer (pH 5.0, 10 mM) and 6.25×10^{-5} moles of EDC. The mixture was stirred overnight followed by the addition of 300 μL of 0.1% (by volume) Tween in PBS to the beads followed by centrifugation. The supernatant was removed, and an additional 500 μL of 0.1% (by volume) Tween in PBS was added and beads were stored at 5 °C.

Target Strand Hybridization and Subsequent Detection. The hybridization process was studied using Becton-Dickson FACS-Calibur flow cytometry system using FL1 (detects 520 ± 40 nm bandwidth), FL2 (detects 585 ± 42 nm bandwidth), and FL4 (detects 661 ± 16 nm bandwidth) detectors. The required compensation was also done.

Kinetic Study. One million QD barcodes 4, 6, and 8 were conjugated to 10 pmol of C4, C6, and C8, respectively. For the singleplex assay, in a volume of 200 μL PBS containing 0.1% Tween, approximately 1.0×10^5 number of microbeads (approximate number of beads were counted in automated Vi-cell counter) of C4 strand conjugated QD barcode 4 was suspended. In the next step, corresponding T4 target strands (1 pmol) as well as SA (5 pmol) were added in the barcode sample simultaneously at room temperature, and the sample was subjected to flow cytometry detection. The time point of addition of the target and SA was regarded as time zero, and the fluorescence obtained from the hybridization process was recorded at every 10 s. For multiplex assay, same procedure was carried out involving QD barcodes 4 and 6 with T4, T6, and SA (2-plex) and QD barcodes 4, 6, and 8 with T4, T6, T8, and SA (3-plex). The kinetics plot was obtained by recording fluorescence against time (s).

Sensitivity Measurements. For singleplex assay, approximately 1 million of QD barcode 4 were conjugated with 1 pmol, 10 pmol, and 60 pmol of C4 capture strands. Sensitivity plots were obtained from hybridization with different amounts of target strands (T4) for each of the above capture strand coverage. For details of the sensitivity experiments for singleplex and multiplex assay see Supporting Information.

Cross-Reactivity Study. All nine QD barcodes were conjugated with their corresponding capture strands shown in Table 1. The surface coverage used was 10 pmol of capture strands added per million of barcodes for each type. For details of the experiment see Supporting Information.

Acknowledgment. We acknowledge the Natural Sciences and Engineering Research Council, Canadian Institute of Health Research, Canadian Foundation for Innovation, Ontario Innovation Trust, Canadian Research Chair's Program for Funding support for the project. We thank D. Li for the preparation of the quantum dots.

Supporting Information Available: Detection intensities of a target as a function of DNA capture strand density on bead surface, detailed methods of sensitivity measurements, and cross-reactivity study. This material is available free of charge *via* the Internet at http://pubs.acs.org.

REFERENCES AND NOTES

1. Hauck, T. S.; Giri, S.; Gao, Y.; Chan, W. C. W. Nanotechnology Diagnostics for Infectious Diseases Prevalent in Developing Countries. *Adv. Drug Delivery Rev.* **2010,** *62*, 438–448.
2. Lopez Alan, D.; Mathers Colin, D.; Ezzati, M.; Jamison Dean, T.; Murray Christopher, J. L. Global and Regional Burden of Disease and Risk Factors, 2001: Systematic Analysis of Population Health Data. *Lancet* **2006,** *367*, 1747–1757.
3. Hufnagel, L.; Brockmann, D.; Geisel, T. Forecast and Control of Epidemics in a Globalized World. *Proc. Natl. Acad. Sci. U. S.A.* **2004,** *101*, 15124–15129.
4. Kingsmore, S. F. Multiplexed Protein Measurement: Technologies and Applications of Protein and Antibody Arrays. *Nat. Rev. Drug Discovery* **2006,** *5*, 310–320.
5. Wongsrichanalai, C.; Barcus Mazie, J.; Muth, S.; Sutamihardja, A.; Wernsdorfer Walther, H. A Review of Malaria Diagnostic Tools: Microscopy and Rapid Diagnostic Test (RDT). *Am. J. Trop. Med. Hyg.* **2007,** *77*, 119–127.

6. Godreuil, S.; Tazi., L.; Banuls, A.-L. In *Encyclopedia of Infectious Diseases: Modern Methodologies*; John Wiley & Sons: New York, 2007; pp 1−30.
7. Mackay, I. M. Real-Time PCR in The Microbiology Laboratory. *Clin. Microbiol. Infect.* **2004,** *10*, 190–212.
8. Schweitzer, B.; Kingsmore, S. Combining Nucleic Acid Amplification and Detection. *Curr. Opin. Biotechnol.* **2001,** *12*, 21–27.
9. Halford, W. P. The Essential Prerequisites for Quantitative RT-PCR. *Nat. Biotechnol.* **1999,** *17*, 835.
10. Sutthent, R.; Gaudart, N.; Chokpaibulkit, K.; Tanliang, N.; Kanoksinsombath, C.; Chaisilwatana, P. p24 Antigen Detection Assay Modified with a Booster Step for Diagnosis and Monitoring of Human Immunodeficiency Virus Type 1 Infection. *J. Clin. Microbiol.* **2003,** *41*, 1016–1022.
11. Klostranec, J. M.; Xiang, Q.; Farcas, G. A.; Lee, J. A.; Rhee, A.; Lafferty, E. I.; Perrault, S. D.; Kain, K. C.; Chan, W. C. W. Convergence of Quantum Dot Barcodes with Microfluidics and Signal Processing for Multiplexed High-Throughput Infectious Disease Diagnostics. *Nano Lett.* **2007,** *7*, 2812–2818.
12. Yager, P.; Edwards, T.; Fu, E.; Helton, K.; Nelson, K.; Tam, M. R.; Weigl, B. H. Microfluidic Diagnostic Technologies for Global Public Health. *Nature* **2006,** *442*, 412–418.
13. Fulton, R. J.; McDade, R. L.; Smith, P. L.; Kienker, L. J.; Kettman, J. R., Jr. Advanced Multiplexed Analysis with The Flow Metrix System. *Clin. Chem.* **1997,** *43*, 1749–1756.
14. Han, M.; Gao, X.; Su, J. Z.; Nie, S. Quantum-Dot-Tagged Microbeads for Multiplexed Optical Coding of Biomolecules. *Nat. Biotechnol.* **2001,** *19*, 631–635.
15. Dejneka, M. J.; Streltsov, A.; Pal, S.; Frutos, A. G.; Powell, C. L.; Yost, K.; Yuen, P. K.; Muller, U.; Lahiri, J. Rare Earth-Doped Glass Microbarcodes. *Proc. Natl. Acad. Sci. U.S.A.* **2003,** *100*, 389–393.
16. Lutz, B. R.; Dentinger, C. E.; Nguyen, L. N.; Sun, L.; Zhang, J.; Allen, A. N.; Chan, S.; Knudsen, B. S. Spectral Analysis of Multiplex Raman Probe Signatures. *ACS Nano* **2008,** *2*, 2306–2314.
17. Nicewarner-Pena, S. R.; Freeman, R. G.; Reiss, B. D.; He, L.; Pena, D. J.; Walton, I. D.; Cromer, R.; Keating, C. D.; Natan, M. J. Submicrometer Metallic Barcodes. *Science* **2001,** *294*, 137–141.
18. Fenniri, H.; Chun, S.; Ding, L.; Zyrianov, Y.; Hallenga, K. Preparation, Physical Properties, On-Bead Binding Assay and Spectroscopic Reliability of 25 Barcoded Polystyrene−Poly(ethylene glycol) Graft Copolymers. *J. Am. Chem. Soc.* **2003,** *125*, 10546–10560.
19. Pregibon, D. C.; Doyle, P. S. Optimization of Encoded Hydrogel Particles for Nucleic Acid Quantification. *Anal. Chem.* **2009,** *81*, 4873–4881.
20. Nam, J.-M.; Stoeva, S. I.; Mirkin, C. A. Bio-Bar-Code-Based DNA Detection with PCR-like Sensitivity. *J. Am. Chem. Soc.* **2004,** *126*, 5932–5933.
21. Wilson, R.; Cossins, A. R.; Spiller, D. G. Encoded Microcarriers for High-Throughput Multiplexed Detection. *Angew. Chem., Int. Ed.* **2006,** *45*, 6104–6117.
22. Finkel, N. H.; Lou, X.; Wang, C.; He, L. Barcoding The Microworld. *Anal. Chem.* **2004,** *76*, 352A–359A.
23. Chan, W. C. W.; Nie, S. Quantum Dot Bioconjugates for Ultrasensitive Nonisotopic Detection. *Science* **1998,** *281*, 2016–2018.
24. Fournier-Bidoz, S.; Jennings, T. L.; Klostranec, J. M.; Fung, W.; Rhee, A.; Li, D.; Chan, W. C. W. Facile and Rapid One-Step Mass Preparation of Quantum-Dot Barcodes. *Angew. Chem., Int. Ed.* **2008,** *47*, 5577–5581.
25. Defoort, J. P.; Martin, M.; Casano, B.; Prato, S.; Camilla, C.; Fert, V. Simultaneous Detection of Multiplex-Amplified Human Immunodeficiency Virus Type 1 RNA, Hepatitis C Virus RNA, and Hepatitis B Virus DNA Using a Flow Cytometer Microsphere-Based Hybridization Assay. *J. Clin. Microbiol.* **2000,** *38*, 1066–1071.
26. Snounou, G.; Viriyakosol, S.; Zhu, X. P.; Jarra, W.; Pinheiro, L.; Do Rosario, V. E.; Thaithong, S.; Brown, K. N. High Sensitivity of Detection of Human Malaria Parasites by The Use of Nested Polymerase Chain Reaction. *Mol. Biochem. Parasitol.* **1993,** *61*, 315–320.
27. Burstain, J. M.; Grimprel, E.; Lukehart, S. A.; Norgard, M. V.; Radolf, J. D. Sensitive Detection of Treponema Pallidum by Using The Polymerase Chain Reaction. *J. Clin. Microbiol.* **1991,** *29*, 62–69.
28. Stoeva, S. I.; Lee, J.-S.; Thaxton, C. S.; Mirkin, C. A. Multiplexed DNA Detection with Biobarcoded Nanoparticle Probes. *Angew. Chem., Int. Ed.* **2006,** *45*, 3303–3306.
29. He, M. X.; Li, K.; Xiao, J. H.; Zhou, Y. X. Rapid Bio-Barcode Assay for Multiplex DNA Detection Based on Capillary DNA Analyzer. *J. Virol. Methods* **2008,** *151*, 126–131.
30. Li, H.; Lau, C.; Lu, J. Carrier-Resolved Technology for Homogeneous and Multiplexed DNA Assays in a One-Pot Reaction. *Analyst* **2008,** *133*, 1229–1236.
31. Cao, Y.-C.; Huang, Z.-L.; Liu, T.-C.; Wang, H.-Q.; Zhu, X.-X.; Wang, Z.; Zhao, Y.-D.; Liu, M.-X.; Luo, Q.-M. Preparation of Silica Encapsulated Quantum Dot Encoded Beads for Multiplex Assay and Its Properties. *Anal. Biochem.* **2006,** *351*, 193–200.
32. Johnson, P. H.; Walker, R. P.; Jones, S. W.; Stephens, K.; Meurer, J.; Zajchowski, D. A.; Luke, M. M.; Eeckman, F.; Tan, Y.; Wong, L.; *et al.* Multiplex Gene Expression Analysis for High-Throughput Drug Discovery: Screening and Analysis of Compounds Affecting Genes Over-Expressed in Cancer Cells. *Mol. Cancer Ther.* **2002,** *1*, 1293–1304.
33. Harraway, J. R.; Smith, M. P.; George, P. M. A Highly Informative, Multiplexed Assay for The Indirect Detection of Hemophilia A Using Five-Linked Microsatellites. *J. Thromb. Haemostasis* **2006,** *4*, 587–590.
34. Moser, M. J.; Christensen, D. R.; Norwood, D.; Prudent, J. R. Multiplexed Detection of Anthrax-Related Toxin Genes. *J. Mol. Diagn.* **2006,** *8*, 89–96.
35. Diebold, R.; Barteit-Kirbach, B.; Evans, D. G.; Kaufmann, D.; Hanemann, C. O. Sensitive Detection of Deletions of One or More Exons in The Neurofibromatosis Type 2 (NF2) Gene by Multiplexed Gene Dosage Polymerase Chain Reaction. *J. Mol. Diagn.* **2005,** *7*, 97–104.
36. Garcia, E. P.; Dowding, L. A.; Stanton, L. W.; Slepnev, V. I. Scalable Transcriptional Analysis Routine—Multiplexed Quantitative Real-Time Polymerase Chain Reaction Platform for Gene Expression Analysis and Molecular Diagnostics. *J. Mol. Diagn.* **2005,** *7*, 444–454.
37. Jennings, T. L.; Rahman, K. S.; Fournier-Bidoz, S.; Chan, W. C. W. Effects of Microbead Surface Chemistry on DNA Loading and Hybridization Efficiency. *Anal. Chem.* **2008,** *80*, 2849–2856.
38. Gao, Y.; Wolf, L. K.; Georgiadis, R. M. Secondary Structure Effects on DNA Hybridization Kinetics: a Solution *versus* Surface Comparison. *Nucleic Acids Res.* **2006,** *34*, 3370–3377.
39. Peterlinz, K. A.; Georgiadis, R. M.; Herne, T. M.; Tarlov, M. J. Observation of Hybridization and Dehybridization of Thiol-Tethered DNA Using Two-Color Surface Plasmon Resonance Spectroscopy. *J. Am. Chem. Soc.* **1997,** *119*, 3401–3402.
40. Wong, E. L. S.; Chow, E.; Gooding, J. J. DNA Recognition Interfaces: The Influence of Interfacial Design on The Efficiency and Kinetics of Hybridization. *Langmuir* **2005,** *21*), 6957–6965.
41. Xu, H.; Sha, M. Y.; Wong, E. Y.; Uphoff, J.; Xu, Y.; Treadway, J. A.; Truong, A.; O'Brien, E.; Asquith, S.; Stubbins, M.; *et al.* Multiplexed SNP Genotyping Using The Qbead System: A Quantum Dot-Encoded Microsphere-Based Assay. *Nucleic Acids Res.* **2003,** *31*, e43/1–e43/10.
42. Gao, Y.; Stanford, W. L.; Chan, W. C. W. Quantum Dot Encoded Microbeads for Multiplexed Genetic Detection of Non-amplified DNA Samples. *Small.* **2011,** *7*, 137–146.
43. Peng, X.; Schlamp, M. C.; Kadavanich, A. V.; Alivisatos, A. P. Epitaxial Growth of Highly Luminescent CdSe/CdS Core/Shell Nanocrystals with Photostability and Electronic Accessibility. *J. Am. Chem. Soc.* **1997,** *119*, 7019–7029.
44. Hines, M. A.; Guyot-Sionnest, P. Synthesis and Characterization of Strongly Luminescing ZnS-Capped CdSe Nanocrystals. *J. Phys. Chem.* **1996,** *100*, 468–471.
45. Dabbousi, B. O.; Rodriguez-Viejo, J.; Mikulec, F. V.; Heine, J. R.; Mattoussi, H.; Ober, R.; Jensen, K. F.; Bawendi, M. G. (CdSe)ZnS Core-Shell Quantum Dots: Synthesis and Optical and Structural Characterization of a Size Series of Highly Luminescent Materials. *J. Phys. Chem. B* **1997,** *101*), 9463–9475.